

# Synthesis and Structural Characterization of a New System: $\text{ZrO}_2\text{--Y}_2\text{O}_3\text{--RuO}_2$

E. Djurado, C. Roux & A. Hammou

Laboratoire d'Ionique et d'Electrochimie du Solide de Grenoble, associé au CNRS (URA 1213), ENSEEG, BP 75, 38402 Saint Martin d'Hères Cedex, France

(Received 20 September 1995; revised version received 25 October 1995; accepted 7 November 1995)

## Abstract

New compounds belonging to the pseudo-ternary system  $\text{ZrO}_2\text{--Y}_2\text{O}_3\text{--RuO}_2$  have been synthesized from nitrates as precursors. The general formula was  $[(\text{ZrO}_2)_{0.91}(\text{Y}_2\text{O}_3)_{0.09}]_{1-x}(\text{RuO}_2)_x$  with  $0 \leq x \leq 20 \text{ mol\% RuO}_2$ . In order to avoid thermal decomposition and to obtain the best sample crystallinity, the last firing was performed at  $900^\circ\text{C}$ . X-ray diffraction measurements provide evidence of a solid solution limit at  $10 \leq x < 12.5 \text{ mol\% RuO}_2$  with the cubic fluorite-type structure. Microstructural analyses show samples with high porosity and heterogeneity in grain size and ruthenium composition.

De nouveaux composés appartenant au système pseudo-ternaire  $\text{ZrO}_2\text{--Y}_2\text{O}_3\text{--RuO}_2$  ont été synthétisés à partir des nitrates comme précurseurs. La formule générale était  $[(\text{ZrO}_2)_{0.91}(\text{Y}_2\text{O}_3)_{0.09}]_{1-x}(\text{RuO}_2)_x$  avec  $0 \leq x \leq 20 \text{ mol\% RuO}_2$ . Dans le but d'éviter la décomposition thermique et d'obtenir la meilleure cristallinité de l'échantillon, le dernier recuit a été effectué à  $900^\circ\text{C}$ . Des mesures de diffraction des rayons X ont permis de mettre en évidence une solution solide dont la limite a été déterminée à  $10 \leq x < 12.5 \text{ mol\% RuO}_2$  dont la structure est cubique de type fluorine. Des analyses microstructurales montrent des échantillons avec une grande porosité et une hétérogénéité en granulométrie et en composition du ruthénium.

## 1 Introduction

Ruthenium oxide  $\text{RuO}_2$  is a transition metal dioxide with a rutile-type structure. Its thermal dissociation is described by the reaction



at  $1461^\circ\text{C}$  under  $0.21 \text{ atm } p\text{O}_2$ .<sup>1</sup> Furthermore,  $\text{RuO}_2$  is considered one of the main active components in so-called dimensionally stable anodes due

to its remarkable electrocatalytic properties.<sup>2</sup> It is well known that its anodic overpotential for oxygen evolution is very low.<sup>3–5</sup> For these reasons, we thought that it would be worthwhile to use it as an electrode in oxygen sensors and solid oxide fuel cells in the form of a  $\text{ZrO}_2\text{--Y}_2\text{O}_3\text{--RuO}_2$  solid solution. Taking into account that very few data are available in the literature related to this aspect,<sup>6</sup> many problems were posed: preparation technique,  $\text{RuO}_2$  solubility and phase stability in stabilized zirconia, thermal stability, electrical conductivity, electrode polarization, etc.

The present paper mainly describes the different attempts to prepare a stable solid-state solution, and the structural characteristics of the powdered and sintered material.

## 2 Experimental

Ternary oxide samples of  $\text{ZrO}_2$ ,  $\text{Y}_2\text{O}_3$  and  $\text{RuO}_2$  were prepared to give compositions with  $[(\text{ZrO}_2)_{0.91}(\text{Y}_2\text{O}_3)_{0.09}]_{1-x}(\text{RuO}_2)_x$ ,  $0 \leq x \leq 20 \text{ mol\% RuO}_2$ . In the following, yttria-stabilized zirconia–ruthenia will be labelled  $\text{YSZRu}_x$ . Samples were prepared from a stoichiometric mixture of ruthenium nitrosyl nitrate  $\text{Ru}(\text{NO})(\text{NO}_3)_3$ , zirconyl nitrate  $\text{ZrO}(\text{NO}_3)_2$  and yttrium nitrate  $\text{Y}(\text{NO}_3)_3$  dissolved in water. The solution was then dried under continuous stirring at  $100^\circ\text{C}$  until total evaporation of water. The products were calcinated at  $500^\circ\text{C}$  for 6 h to decompose the nitrates. The complete thermal decomposition of the nitrates used as precursors was observed at  $500^\circ\text{C}$  by thermogravimetry using a Netzsch Thermal Analyser (Fig. 1). This result is in agreement with those reported by Ardizzone *et al.*<sup>7</sup> concerning the decomposition of  $\text{Ru}(\text{NO})(\text{NO}_3)_3$ .

After pyrolysis at  $500^\circ\text{C}$ , subsequent grinding and annealing of the sample was undertaken at different temperatures—800, 900, 1100 and  $1400^\circ\text{C}$ —to investigate its thermal stability. Firings were carried out in air at a heating rate of  $5^\circ\text{C min}^{-1}$  for 12 h

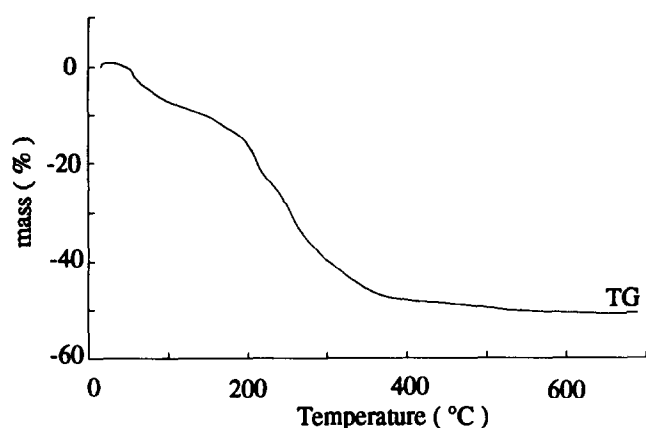


Fig. 1. Thermogravimetric analysis of  $\text{ZrO}(\text{NO}_3)_2 + \text{Y}(\text{NO}_3)_3 + \text{Ru}(\text{NO})(\text{NO}_3)_3$ .

duration at each temperature. Samples were furnace-cooled to room temperature.

Note that two further preparation methods were used in unsuccessful attempts to synthesize a new single phase with YSZ/ $\text{RuO}_2$ .  $\text{RuO}_2$  was mixed with different yttria-stabilized zirconia (YSZ) materials:

- (1) commercially available YSZ powder (9 mol%  $\text{Y}_2\text{O}_3$ , from Tosoh) and
- (2) YSZ powder prepared from calcination of Zr and Y hydroxides at  $500^\circ\text{C}$ . The mixture of Zr and Y hydroxides was obtained using the butylate method.<sup>8</sup>

These methods, based on the solid-state route, led to a two-phase mixture of  $\text{RuO}_2$  and YSZ.

YSZ $\text{Ru}_x$  powder was pressed in a uniaxial die at  $1500 \text{ kg cm}^{-2}$  to form a pellet (12.8 mm in diameter and 3.1 mm thick). X-ray characterization at room temperature was carried out using a Siemens D500 diffractometer equipped with a linear detector (Cu  $K_{\alpha 1}$  radiation,  $\lambda = 1.5406 \text{ \AA}$ ). Silicon was used as the internal reference for all scans ( $0.04^\circ$ ,  $2\theta$  steps, 5 s counting time).

Scanning electron microscopy (SEM) and electron probe micro analysis (EPMA) (Cameca SX50) were performed to characterize the crystal microstructure. Two YSZ $\text{Ru}_{10}$  samples synthesized at 900 and  $1400^\circ\text{C}$  were studied by EPMA. Four elements were analysed: standard no. 1 is pure Ru calibrated on line  $L_{\alpha}$  at 15 kV using a polyethylene terephthalate (PET) ( $\text{C}_5\text{H}_{12}\text{O}_4$ ) crystal; standard no. 2 is Zr in YSZ (wt% = 62.67) calibrated on line  $L_{\beta}$  at 15 kV using a PET crystal and not on the  $L_{\alpha}$  in order to avoid overlap of the Y  $L_{\beta}$ ; standard no. 3 is Y in YSZ (wt% = 12.08) calibrated on line  $L_{\alpha}$  at 15 kV with a thallium acid phthalate (TAP) ( $\text{C}_8\text{H}_5\text{O}_4\text{Ti}$ ) crystal; standard no. 4 is O in YSZ (wt% = 25.25) calibrated on line  $K_{\alpha}$  at 15 kV with a PCl multilayer (W-Si) crystal. Note that Zr, Y and O standards come from the nominal  $(\text{ZrO}_2)_{0.91}(\text{Y}_2\text{O}_3)_{0.09}$  composition which was

prepared via nitrates up to  $1400^\circ\text{C}$  and gave satisfactory quantitative results compared with calculated values.

### 3 Results and Discussion

The first section deals with the new material prepared as a powder and the second part with the new material prepared as sintered ceramics.

#### 3.1 YSZ $\text{Ru}_x$ powder

The firing procedure (successive grinding and annealing) proved to be essential to keep the  $\text{RuO}_2$  in the yttria-stabilized zirconia matrix giving rise to a black compound. The main advantage of the nitrate method compared with the classical solid-state reaction route is that it stabilizes  $\text{RuO}_2$  in solid solution at low temperatures, which otherwise decomposes into Ru and  $\text{RuO}_4$  at temperatures higher than  $1000^\circ\text{C}$ .<sup>9</sup> The minimum temperature at which  $\text{RuO}_2$  could be incorporated into YSZ was  $500^\circ\text{C}$ .

X-ray diffraction patterns of YSZ $\text{Ru}_x$  compounds with  $0 \leq x \leq 10$ , fired at  $500^\circ\text{C}$ , showed one single cubic phase, similar to that of YSZ, with very broad peaks indicating poor crystallinity. To improve the crystallinity of the compounds, treatments were carried out at 800 and  $900^\circ\text{C}$ . These firings yielded well-crystallized monophase samples. A typical XRD pattern of the YSZ $\text{Ru}_{10}$  powder after a  $900^\circ\text{C}$  treatment for 12 h is shown in Fig. 2. Based on this profile, a cubic fluorite-related structure could be assigned to YSZ $\text{Ru}_{10}$  solid solution. The unit-cell parameter changed from 0.5129(3) nm for pure YSZ to 0.5098(2) nm for YSZ $\text{Ru}_{10}$  solid solution.

The influence of temperature on the variation of full width at half maximum (FWHM) of the (220) peak for YSZ $\text{Ru}_{2.5}$  was investigated. FWHM values of  $0.81^\circ$ ,  $0.73^\circ$  and  $0.49^\circ$  ( $\pm 0.04^\circ$ ) were found at

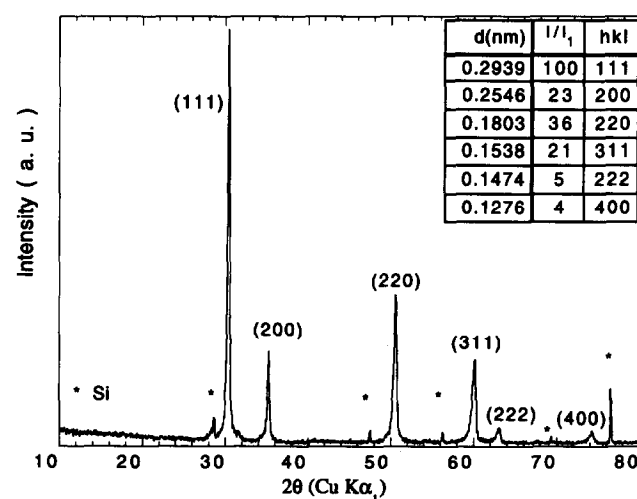


Fig. 2. Typical X-ray powder diffraction pattern of  $[(\text{ZrO}_2)_{0.91}(\text{Y}_2\text{O}_3)_{0.09}]_{0.9}(\text{RuO}_2)_{0.1}$  fired at  $900^\circ\text{C}$ .

500, 800 and 900°C, respectively. The decrease in FWHM with increasing temperature is consistent with a better crystallinity and larger grain size.

To study the chemical stability of the new oxides with temperature, special attention was paid to the temperature dependence of the (1 1 1) and (2 0 0) reflections of  $\text{YSZRu}_{10}$  sintered at 800, 900, 1100 and 1400°C (Fig. 3). The (1 1 1) peak of pure  $\text{RuO}_2$  appears at 1100°C, indicating the thermal decomposition of the solid solution. At 1400°C, the X-ray profile is quite similar to that of pure YSZ.

In Fig. 4, simultaneous examination of the (1 1 1) and (2 0 0) positions indicates a  $2\theta$  shift towards lower angles from 1000°C due to the loss of ruthenium and recovering of the YSZ configuration. In an oxidizing atmosphere, during the volatilization of  $\text{RuO}_2$ , Bell and Tagami<sup>10</sup> reported that the main vapour species are  $\text{RuO}_3$  and  $\text{RuO}_4$  in the range 1465 to 2090°C. We may conclude that the best compromise between thermal stability and crys-

tallinity appears to be achieved with calcination at 900°C.

To determine the solubility limit of  $\text{RuO}_2$  in YSZ, samples containing 2.5, 5, 10, 12.5, 15 and 20 mol%  $\text{RuO}_2$  were prepared. Up to 10 mol%  $\text{RuO}_2$ , all the samples were single phase with the cubic fluorite-type structure. For higher  $\text{RuO}_2$  content, peaks characteristic of the excess of  $\text{RuO}_2$  appeared, indicating that the limit of the solid solution was reached between 10 and 12.5 mol%  $\text{RuO}_2$  (Fig. 5).

In the solid solution domain, the lattice parameter variation (Fig. 6) follows the linear relationship:

$$a \text{ (nm)} = 0.5128(6) - 0.2(8) \times 10^{-3} x$$

These data suggest that the contraction of the unit cell is correlated to  $\text{RuO}_2$  dissolution in YSZ.  $\text{Ru}^{4+}$  is six-fold coordinated in its rutile structure and has an ionic radius of 0.62 Å. In the YSZ,  $\text{Zr}^{4+}$  is eight-fold coordinated and its ionic radius is 0.84 Å.<sup>11</sup> Thus, it is not ruled out that  $\text{Ru}^{4+}$  could be

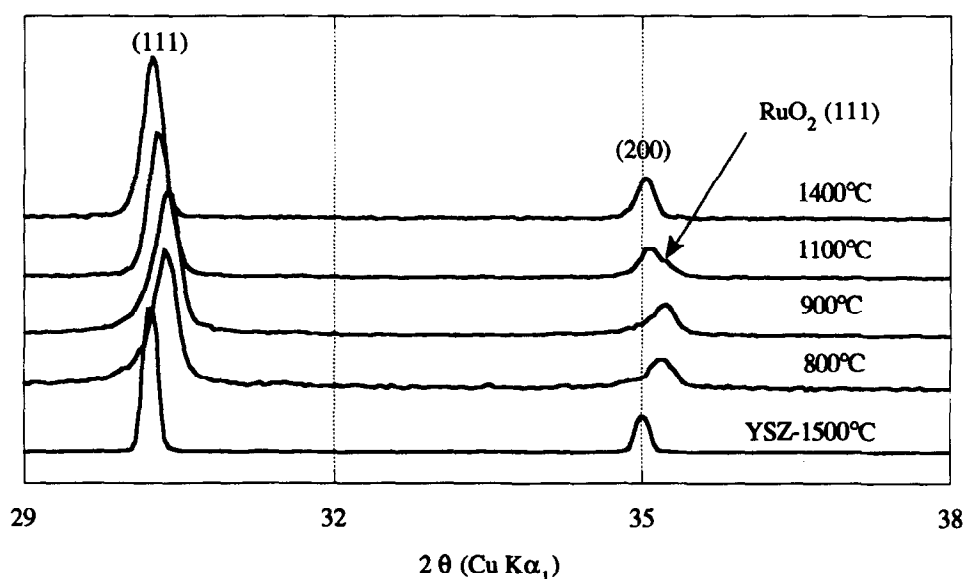


Fig. 3. Temperature dependence of the (1 1 1) and (2 0 0) X-ray positions of YSZ/10 mol%  $\text{RuO}_2$ .

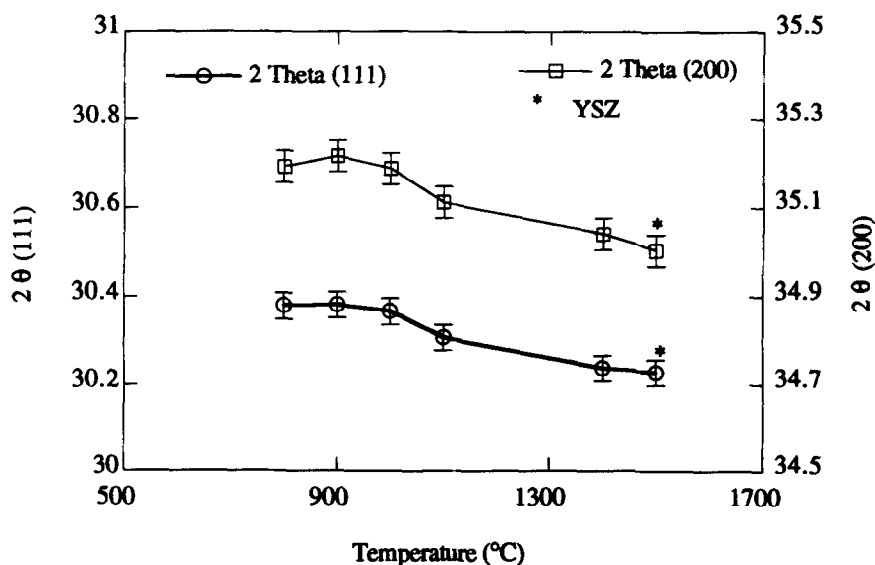


Fig. 4. The  $2\theta$  shifting with temperature of the (1 1 1) and (2 0 0) X-ray positions of YSZ/10 mol%  $\text{RuO}_2$ .

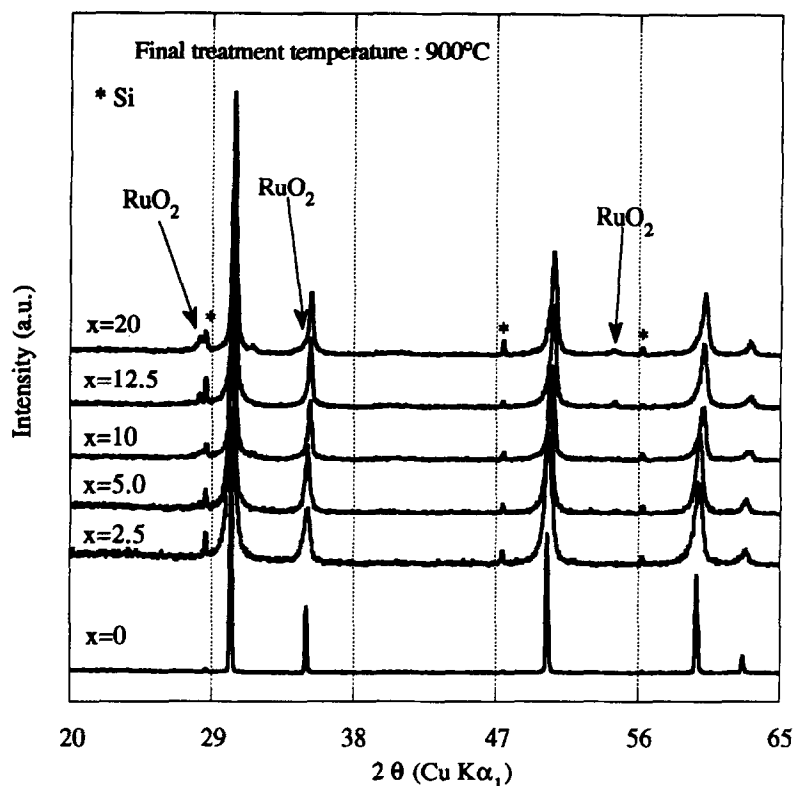


Fig. 5. X-ray diffraction spectra as a function of  $x$  mol%  $\text{RuO}_2$  in  $[(\text{ZrO}_2)_{0.91}(\text{Y}_2\text{O}_3)_{0.09}]_{1-x}(\text{RuO}_2)_x$ .

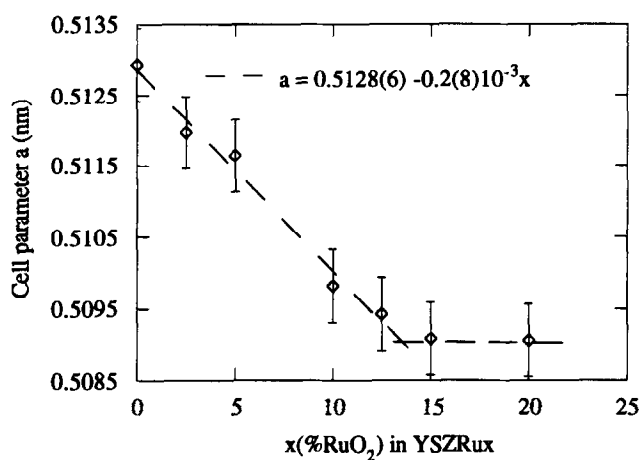


Fig. 6. Variation of the cell parameter with  $\text{RuO}_2$  content in the system  $[(\text{ZrO}_2)_{0.91}(\text{Y}_2\text{O}_3)_{0.09}]_{1-x}(\text{RuO}_2)_x$ .

incorporated in the YSZ matrix as a substitutional dopant on  $\text{Zr}^{4+}$  sites.  $\text{Ru}^{4+}$  may also occupy interstitial sites. X-ray diffraction did not allow us to conclude the nature of the local environment of Ru because the dopant ( $\text{Ru}^{4+}$ ) has an atomic number very close to the doped value ( $\text{Zr}^{4+}$ ). Raman measurements at the  $K$  threshold of ruthenium (22118 eV) are planned to determine the local environment of  $\text{Ru}^{4+}$  in YSZ.

### 3.2 YSZRu<sub>x</sub> ceramics

The final sintering temperature of 900°C and the 12 h sintering duration were selected to avoid thermal decomposition of the solid solution. This was confirmed by X-ray analysis (Fig. 3).

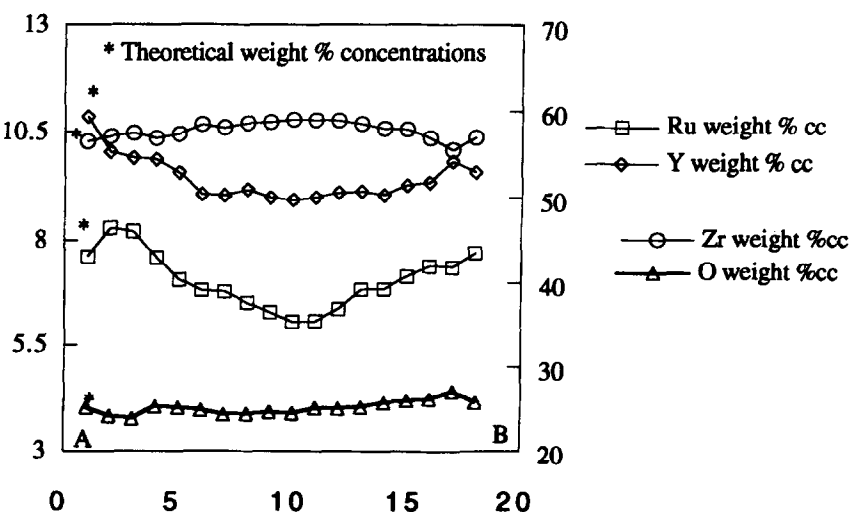


Fig. 7. Change of Ru, Y, Zr and O wt% through the 25  $\mu\text{m}$  grain. A and B are the extremities of this path.

**Table 1.** Quantitative analysis on  $\text{YSZRu}_{10}$  prepared at  $1400^\circ\text{C}$ 

Element	Theoretical wt%	Measured wt%
Ru	7.62	0.42
Zr	56.38	65.30
Y	10.86	8.08
O	25.13	25.73

No shrinkage was found in a dilatometry experiment in air on  $\text{YSZRu}_{10}$  up to  $1000^\circ\text{C}$ . The density of  $\text{YSZRu}_{10}$  pellets sintered at  $900^\circ\text{C}$  for 12 h was  $\sim 3.6 \text{ g cm}^{-3}$ .

Porosity was detected using SEM. In addition, heterogeneity in the grain size (from 1 to  $25 \mu\text{m}$ ) as well as in the composition of particles was observed. A composition profile was determined through the particles of around  $25 \mu\text{m}$  in size. It shows a small gradient of ruthenium composition in the grain (Fig. 7), ruthenium being located on the periphery of the particle.

A sintering study needs to be carried out to increase the density of samples, which is too low at present because of the synthesis technique.

Finally, a microprobe analysis on the  $\text{YSZRu}_{10}$  prepared at  $1400^\circ\text{C}$  in air confirms that a significant amount of ruthenium is lost under these conditions (Table 1).

#### 4 Conclusion

In the present work, new oxides,  $[(\text{ZrO}_2)_{0.91}(\text{Y}_2\text{O}_3)_{0.09}]_{1-x}(\text{RuO}_2)_x$ , belonging to the cubic solid solution with  $0 \leq x < 12.5 \text{ mol}\%$   $\text{RuO}_2$ , have been synthesized by solid-state chemistry from nitrates as precursors. The last  $900^\circ\text{C}$  firing step was carried out to obtain the best possible crystallinity and good

thermal stability of the monophasic fluorite-related compound. The contraction of the unit cell parameter has been correlated to  $\text{RuO}_2$  incorporation into the YSZ matrix. Further work is planned to investigate the local environment of  $\text{Ru}^{4+}$  in the new compounds by Raman spectroscopy and Extended X-ray Absorption Fine Structure (EXAFS).

On the other hand, SEM and EPMA results mainly show heterogeneity in the grain size and ruthenium composition. Moreover, high porosity is observed inside and between grains. Our future experiments will aim at reducing the porosity and enhancing the microstructural homogeneity.

#### Acknowledgement

The authors would like to thank the Commission of the European Communities for their financial support (Project JOUE-004C).

#### References

1. Tagirov, V. K., Chizhikov, D. M., Kazenas, E. K. & Shubochkin, L. K., *J. Inorg. Chem.*, **20** (1977) 1133.
2. Beer, H. B., *J. Electrochem. Soc.*, **127** (1980) 303C.
3. Trasatti, S. & Buzzance G., *J. Electroanal. Chem. Interfacial Electrochem.*, **29** (1971) 635.
4. O'Grady, W., Twakura, C., Huang, J. & Yeager, E., in *Electrocatalysis*, ed. M. W. Breiter. The Electrochemical Society Softbound Symposium Series, Princeton, NJ, 1974, p. 286.
5. Burke, L. D., Murphy, O. J., O'Neill, J. E. & Venkatesan, S., *J. Chem. Soc., Faraday Trans. 1*, **73** (1977) 1659.
6. Long, Y. C., Zhang, Z. D., Dwight, K. & Wold A., *Mater. Res. Bull.*, **23** (1988) 631.
7. Ardizzone, S., Falciola, M. & Trasatti, S., *J. Electrochem. Soc.*, **136** (1989) 1545.
8. Koch, M. & Nair K. M., *Cermugia Int.*, **2**[2] (1976) 88.
9. Pascal P., *Nouveau Traité de Chimie Minérale*. Masson et Cie editors, Paris, Vol. XIX, 1958, p. 85.
10. Bell, W. E. & Tagami, M., *J. Phys. Chem.*, **67**[11] (1963) 2432-6.
11. Shannon, R. D. & Prewitt, C. T., *Acta Cryst.*, **B25** (1969) 925.